Structure-activity relations of rosmarinic acid derivatives for the amyloid β aggregation inhibition and antioxidant properties

Structure–activity relations of rosmarinic acid derivatives for the amyloid β aggregation inhibition and antioxidant properties.

Riho Taguchi[a], Koki Hatayama[a], Tomohito Takahashi[a], Takafumi Hayashi[b], Yuki Sato[b], Daisuke Sato[b], Kiminori Ohta[b], Hiroto Nakano[a], Chigusa Seki[a], Yasuyuki Endo[b], Kiyotaka Tokuraku[a], and Koji Uwai[a*]

a) Division of Sustainable and Environmental Engineering, Graduate School of Engineering, Muroran Institute of Technology, 27-1 Mizumoto, Muroran 050-8585, Japan
b) Tohoku Medical and Pharmaceutical University, 4-4-1 Komatsushima, Aoba-ku, Sendai 981-8558, Japan
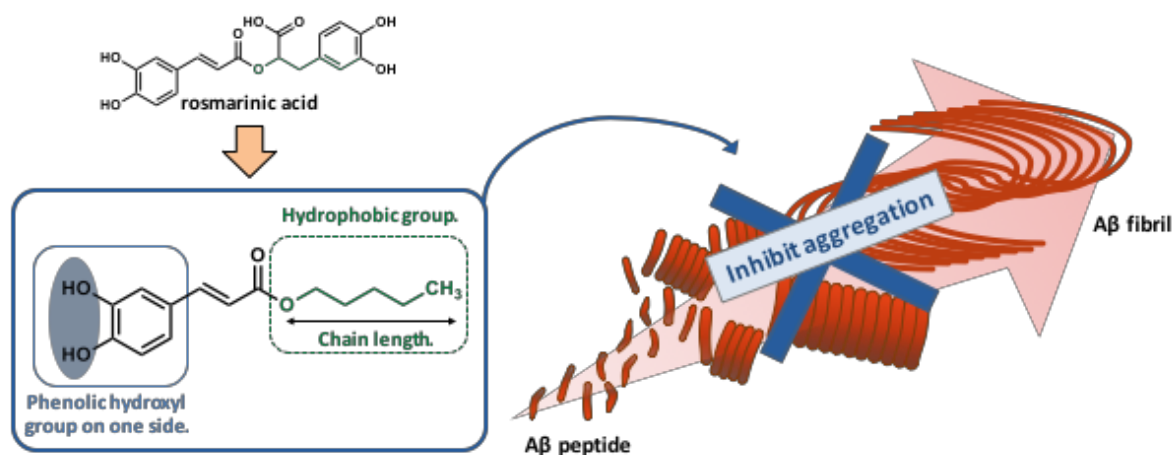
(Corresponding author)
Dr. Koji Uwai
Division of Sustainable and Environmental Engineering, Graduate School of Engineering, Muroran Institute of Technology, 27-1 Mizumoto, Muroran 050-8585, Japan
e-mail: uwai@mmm.muroran-it.ac.jp

Graphical Abstract

Critical functional groups in rosmarinic acid derivatives for Aβ aggregation inhibitory activity

Highlights

• 25 rosmarinic acid derivatives with anti-AD properties have been synthesized

• *In vitro* anti-Aβ aggregation, antioxidant properties, XOD inhibition were evaluated

• Structure–activity relations were discussed

• Compounds **16d** and **19** are the most potent amyloid aggregation inhibitors

Abstract

Amyloid-β aggregation inhibitors are expected to be therapeutic or prophylactic agents for Alzheimer's disease. Rosmarinic acid, which is one of the main aggregation inhibitors derived from *Lamiaceae*, was employed as a lead compound and its 25 derivatives were synthesized. In this study, the structure–activity relations of rosmarinic acid derivatives for the amyloid-β aggregation inhibitory effect (MSHTS assay), antioxidant properties, and xanthine oxidase inhibition were evaluated. Among the tested compounds, compounds **16d** and **19** were found to the most potent amyloid aggregation inhibitors. The SAR revealed that the necessity of the presence of the phenolic hydroxyl on one side of the molecule as well as the lipophilicity of the entire molecule. The importance of these structural properties was also supported by docking simulations.

Key words: Alzheimer's disease, structure–activity relationship, inhibitor, rosmarinic acid, amyloid-beta, aggregation

1. Introduction

Alzheimer's disease (AD) is one of the most common neurodegenerative diseases in late adult life and accounts for 70 percent of dementia. The onset of AD leads to the progressive loss of learning ability and mental, behavioral and functional decline [1]. The number of the patients with AD is estimated to reach 150 million by 2050 due to the acceleration of demographic aging [2]. Choline esterase inhibitors (donepezil, galanthamine, rivastigmine) and an *N*-methyl-D-aspartic acid receptor antagonist (memantine) are now used for the medical treatment of AD. However, these treatments are used only for delaying the progression of AD [3]. Thus, the development of a fundamental AD treatment is becoming increasingly urgent.

In the AD patient's brain, the amyloid β (Aβ) protein is cut out of the amyloid precursor protein by the action of β-secretase and γ–secretase, is oligomerized, and becomes fibrotic by aggregation, finally forming senile plaques. This insoluble Aβ fiber is thought to induce neuronal death and cognitive dysfunction as a result of the deposition of senile plaques formed from the Aβ fiber in the vascular wall in the brain (the Aβ cascade hypothesis) [4]. Thus, Aβ aggregation inhibitors are expected to be therapeutic or prophylactic agents for AD.

Previously, a series of bisphenols [5], alkaloids [6], polyphenols [7], and peptides with C-terminal motif of Aβ [8] have been reported as the target compound Aβ aggregation inhibitors. On the other hand, based on the demonstration of the correlation between the Aβ aggregation inhibitory activity and antioxidant activity [9], it appears that the study of the Aβ aggregation inhibitors based on the polyphenols can make a significant contribution to the development of AD treatment. For example, the relation between the structure of curcumin, an active polyphenol, and the Aβ aggregation inhibitory activity has been well-studied [10,11].

Recently, we established a novel method for the evaluation of the Aβ aggregation inhibitory activity called the "microliter scale high - throughput screening (MSHTS) system" [12], and showed that the results obtained by this method were comparable to those obtained using Thioflavin-T (ThT) assay, which is the standard method for the evaluation of the Aβ aggregation inhibitory activity. Using this new method, we found that of 52 tested spices, a member of *Lamiaceae* showed the strongest activity, and rosmarinic acid (**1**) isolated from *Satureja hortensis* (one of the species of *Lamiaceae* family) was a main Aβ aggregation inhibitor. Additionally, it was reported that rosmarinic acid led to an improvement in the cognitive function in Tg2576 mice [13].

Rosmarinic acid (**1**) is also reported to show a high antioxidant activity [14]. Aβ-induced neuronal toxicity is regulated by the reactive oxygen species (ROS) generation that assists subsequent Aβ aggregation and speeds up the AD progression [15, 16] and antioxidants with catechol moiety showed to inhibit Aβ aggregation [17]. Thus, the relations between antioxidant activity and Aβ aggregation in the viewpoint of the compound structure is also of interest.

Herein, we studied the structure–activity relations between the structures of rosmarinic acid derivatives and the Aβ aggregation inhibitory activity and also performed simulations of the docking of these derivatives with the Aβ monomer. Moreover, their potency as scavengers of the superoxide radical, produced by xanthine oxidase (XOD) (enzymatic method) and by the diphenyl picrylhydrazyl (DPPH) assay (chemical method) were also studied.

2. Results and Discussion

2.1 Chemistry

Rosmarinic acid (**1**) has five key structural groups: a carboxy group, two phenol hydroxy groups, an unsaturated C–C bond, an alkoxy group, and an ester moiety (Fig. 1).
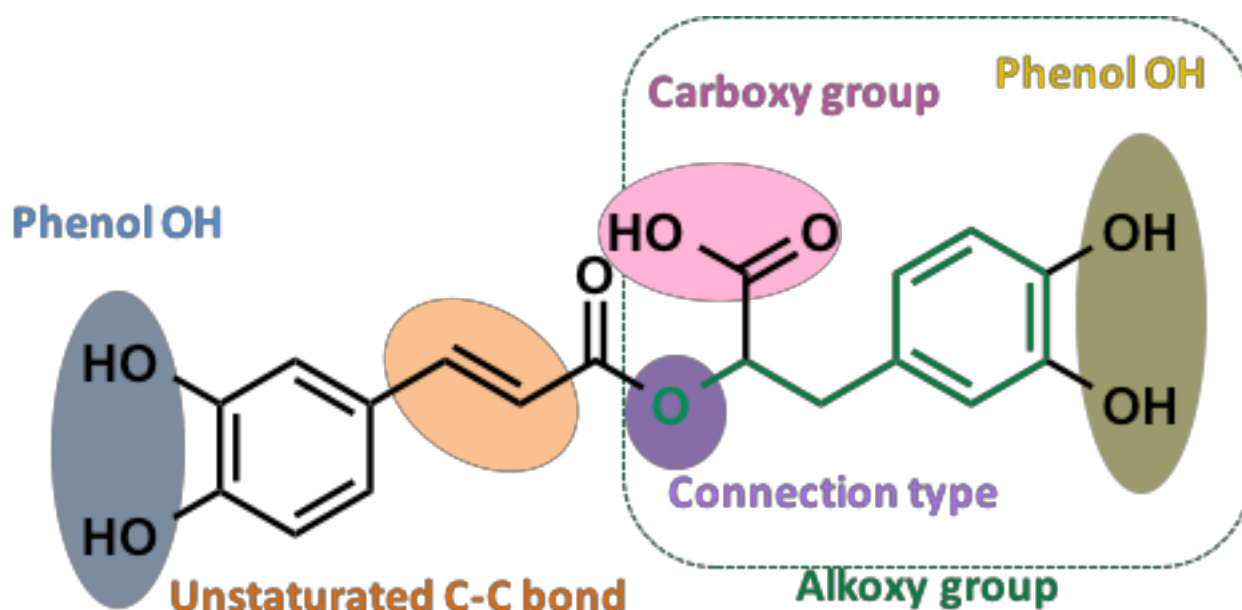
Fig. 1. Key points in the structure of rosmarinic acid (**1**)

Initially, we directed our attention to the carboxy group and prepared two analogs of rosmarinic acid, rosmarinic amide (**2**)[18,19] and caffeic acid 3,4-dihydroxyphenethyl ester (**12c**)[20,21,22] (Scheme 1). Rosmarinic amide (**2**) was synthesized using Won's protocol [18,19]. However, since the yield obtained by this approach was quite poor, we attempted to synthesize it *via* an acid chloride prepared with oxalyl chloride and NH_3 [23]. We attempted to prepare the caffeic acid 3,4-dihydroxyphenethyl ester (**12c**) by the direct Mitsunobu reaction of 3,4-dihydroxyphenethyl alcohol with caffeic acid (**3**); however, the target yield was only 4.8%. Examination of the structure of 3,4-dihydroxyphenethyl alcohol shows that it possesses several alcohol groups that can function as a nucleophile in basic conditions. Additionally, the electrophilicity of the carboxy moiety of caffeic acid (**3**) was decreased because of the conjugation of the phenolic hydroxyls. Therefore, we planned to protect the phenolic hydroxyls in caffeic acid (**3**) and 3,4-dihydroxyphenethyl alcohol. The phenolic hydroxyls of 3,4-dihydroxyphenethyl alcohol were protected with *tert*-butyldimethylsilyl (TBS) groups, and the caffeic acid (**3**) phenolic hydroxyls were protected with the 2-nitrobenzensulfonyl (Ns) groups. NsO-groups exhibit an electron-withdrawing nature, and therefore the electrophilicity of the conjugated carboxy moiety was expected to be increased. In particular, caffeic acid (**3**) was esterified by Fischer's ester synthesis and the phenolic hydroxyls were protected by the Ns groups, with acid hydrolysis of the ester giving carboxylic acid (**6a**). The coupling partner, the protected 3,4-dihydroxyphenethyl alcohol (**10a**), was synthesized from 3, 4-dihydroxyphenylacetic acid (**7**). Allyl esterification of carboxylic acid (**7**) followed by TBS-protection of phenolic hydroxyls and reduction of the ester with lithium aluminum hydride gave alcohol (**10a**). Condensation of the protected carboxylic acid (**6a**) and alcohol (**10a**) followed by the deprotection of Ns and TBS groups gave caffeic acid 3,4-dihydroxyphenethyl ester (**12c**).
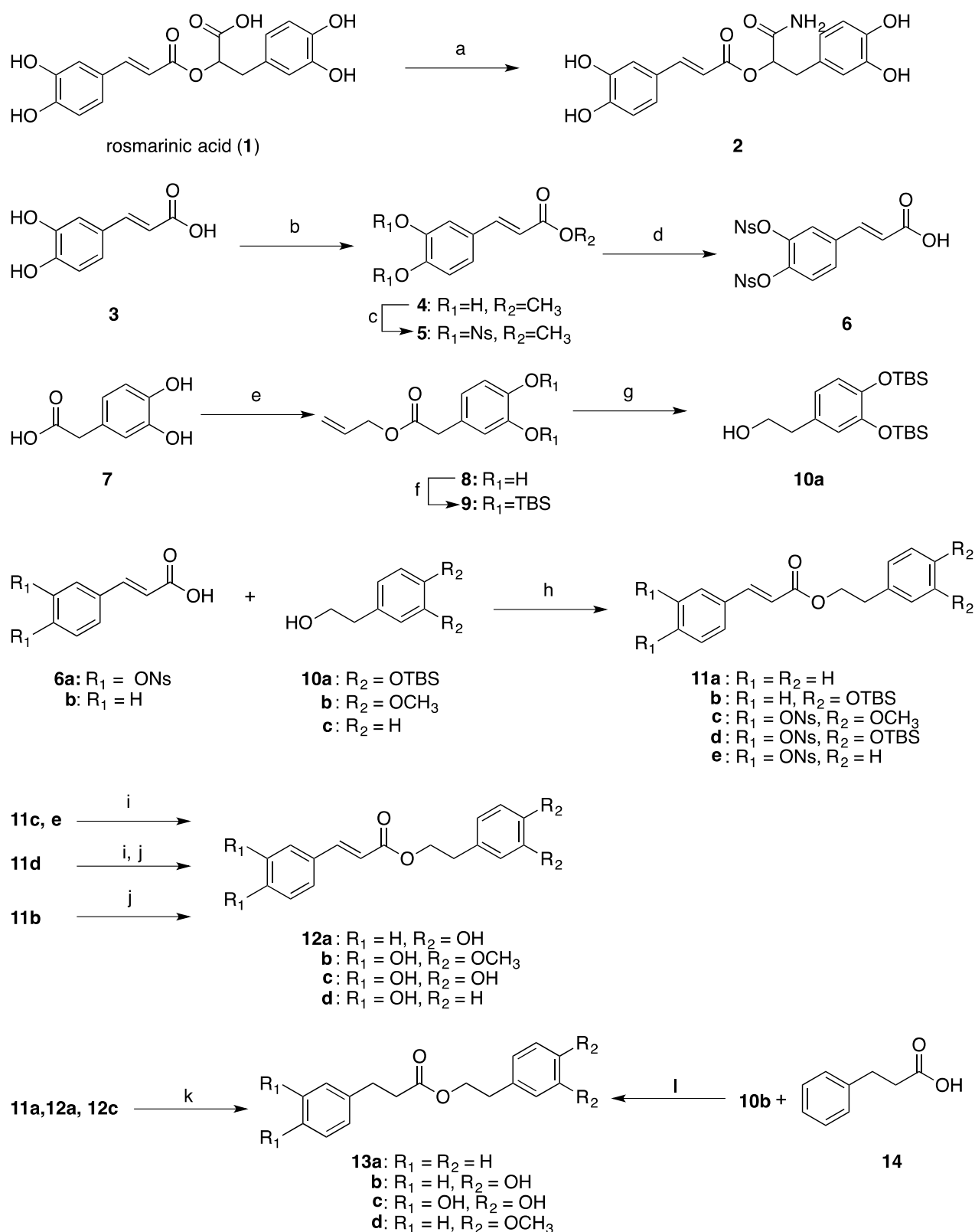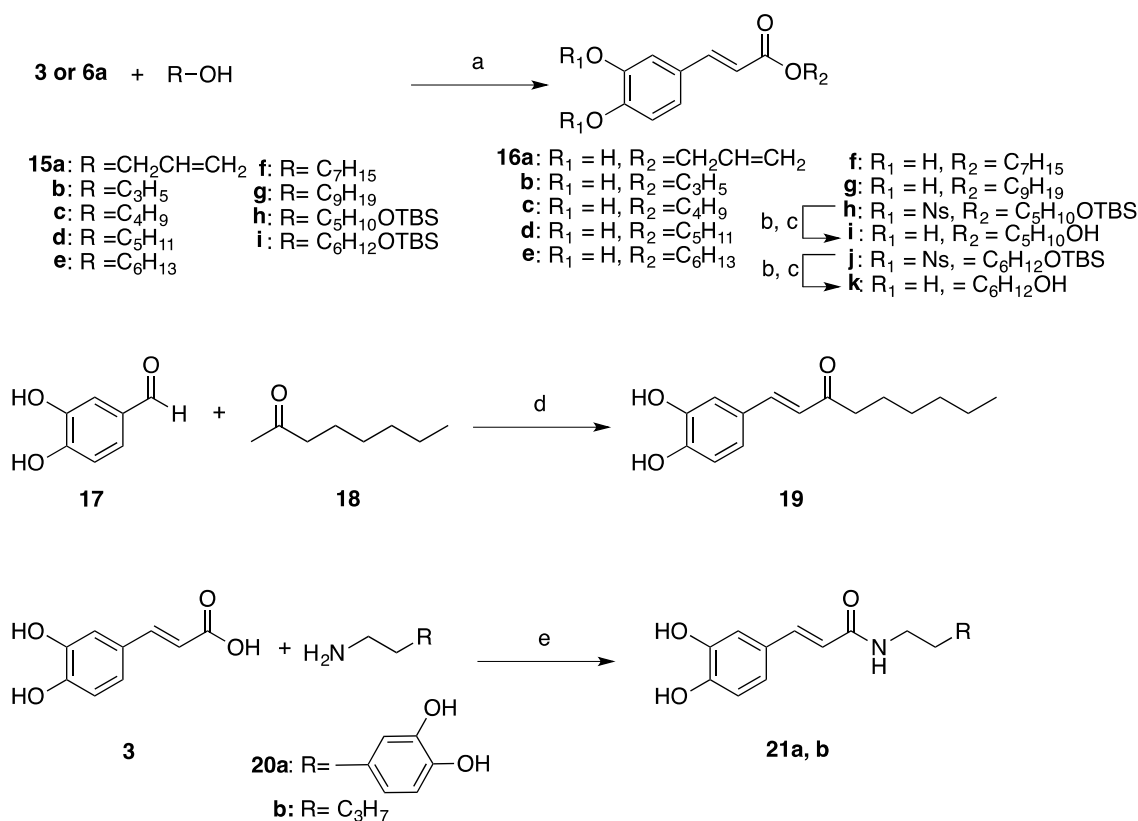
(2-column-fitting image)

Scheme 1. a) oxalyl chloride, NH_3, THF, rt, 19.5 h; b) EDCI, DMAP, MeOH; c) NsCl, Et_3N, CH_3CN; d) AcOH, 0.5 M HCl; e) EDCI, DMAP, Allyl alcohol; f) TBSCl, imidazole, DMF; g) $LiAlH_4$, THF; h) DEAD, TPP, THF, 0 °C → rt; i) PhSH, Cs_2CO_3, CH_3CN, 0 °C → rt; j) TBAF, THF, 0 °C → rt; k) H_2, Pd/C; l) DIAD, TPP, THF, 0 °C → rt

Similarly, to investigate the effect of phenolic hydroxyls and unsaturated C–C bond, a series of carboxylic acids (**6a, b**) and alcohols (**10a-c**) were coupled, followed by deprotection to give esters (**11a, 12a-d**). Unsaturated C–C bond in compound **11a**, **12a**, and **12c** were reduced by catalytic hydrogenation to give compounds **13a-c**.

Caffeic acid alkyl esters (**16a-g, i, k**) were also prepared by the condensation reaction of caffeic acid (**3**) and corresponding alkyl alcohols (**15a-i**) to study the effect of the aromatic ring on one side of the molecule (Scheme 2). Additionally, to confirm the effect of the ester group, ketone (**19**)[24] and amide (**21a, b**) were synthesized.
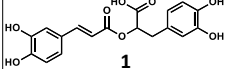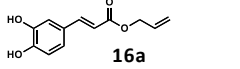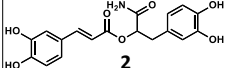

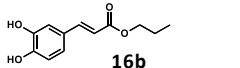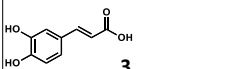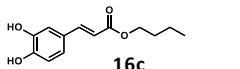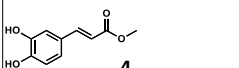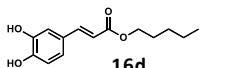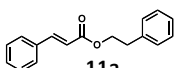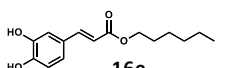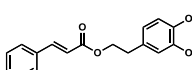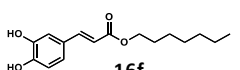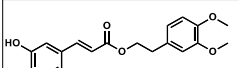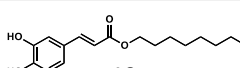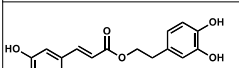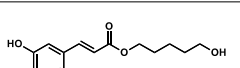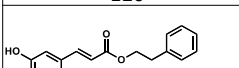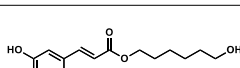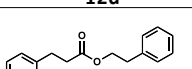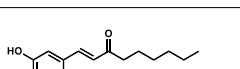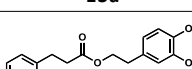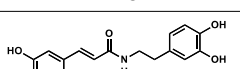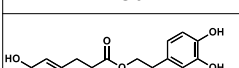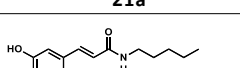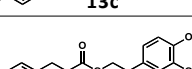(2-column-fitting image)

Scheme 2. a) DIAD, PPh$_3$, THF, r.t.; b) PhSH, Cs$_2$CO$_3$, CH$_3$CN, 0 °C → rt; c) TBAF, THF, 0 °C → rt; d) pyrolidine, AcOH, THF, reflux; e) iPr$_2$NEt, DMAP, EDCI, DMF, rt

2.2 Aβ(1-42) aggregation inhibitory activity

Elucidation of the essential structural factor for the inhibition of the Aβ(1-42) aggregation inhibitory activity would lead to the development of more effective inhibitors and would obtain vital information for the elucidation of the inhibitory action mechanism. Therefore, we directed our attention to the five structural features of rosmarinic acid (**1**) that show the strong activity: carboxy group, phenolic hydroxyls, unsaturated C–C bond, alkoxy group, and ester moiety. We synthesized various derivatives and evaluated their Aβ(1-42) aggregation inhibitory activities (Table 1).

Table 1. Aβ(1−42) aggregation inhibitory activity by MSHTS system and CLogP values of rosmarinic acid derivatives

Compounds	EC$_{50}$ [μM]	CLogP	Compounds	EC$_{50}$ [μM]	CLogP
1	20.3	1.10	16a	23.2	1.98
2	21.9	0.27	16b	24.7	2.26
3	216	0.97	16c	12.0	2.79
4	67.7	1.20	16d	2.58	3.32
11a	1040	4.56	16e	5.13	3.85
12a	7.95	3.30	16f	10.4	4.38
12b	39.5	2.96	16g	9.52	5.43
12c	20.6	2.03	16i	80.1	1.33
12d	8.41	3.30	16k	54.8	1.86
13a	4536	4.38	19	2.82	3.53
13b	5.93	3.11	21a	69.0	1.37
13c	14.9	1.85	21b	11.4	2.66
13d	274	4.03			

First, we studied the effect of carboxy group on the activity. Compared to the Aβ(1-42) aggregation inhibitory activity of rosmarinic acid (**1**, EC$_{50}$ = 20.3 μM), amide (**2**) and compound **12c**, which eliminate the carboxylic acid, showed almost equivalent activities of 21.9 μM and 20.6 μM, respectively. This suggested that the carboxy group did not affect the activity.

Next, the effect of phenolic hydroxyls was evaluated. Compared to the EC$_{50}$ value of compound **12c** (20.6 μM), the EC$_{50}$ values of compound **12a**, for which the phenolic hydroxyls on the carboxylic side were eliminated, and compound **12d**, for which the phenolic hydroxyls on the

alkoxy moiety were eliminated, were 7.95 and 8.41 µM, respectively. Thus, the activity was enhanced by the elimination of phenolic hydroxyls. However, interestingly, compound **11a**, for which the phenolic hydroxyls on both sides were deleted, exhibited the activity of 1,040 µM. These results suggested that lateral phenolic hydroxyls on odd side were important for the activity.

Similarly, compound **12b**, for which the phenolic hydroxyls were masked with methoxyl functional groups, showed significantly lower activity (EC_{50} = 39.5 µM) than compound **12c**. In line with the results described above, in contrast to the activity of compound **13a** (EC_{50} = 4,536 µM), for which the phenolic hydroxyls on both sides were eliminated, compound **13d**, for which hydroxyl groups on the alkoxy side were masked with methoxy groups, showed a higher activity (EC_{50} = 274 µM). Moreover, compound **13b**, for which the hydroxyls were present on the alkoxy side, showed significantly higher activity (EC_{50} = 5.93 µM) than compound **13d**. These results suggested that not only the existence of polar functional groups but also the functional groups that could make hydrogen bonds or were hydrophilic affected the activity.

To evaluate the effect of the aromatic rings on the activity, we tested the compounds for which one phenyl ring was substituted with an alkyl chain. Compound **16** (EC_{50} = 5.13 µM) for which the alkyl chain was as long as that of compound **12d** showed almost the same activity as the parent compound. This result suggested that the existence of the aromatic ring was not important for the activity; rather, the presence of a hydrophobic group in the alkoxy moiety was vital.

Next, the effect of the alcohol substitution for catechol was investigated. The activity of compound **16k** (EC_{50} = 54.8 µM) with alcohol in alkoxy moiety was significantly impaired when compared to compound **12c** with catechol. This result suggested that catechol was important for the activity, seemingly contradicting the interpretation of the results for **16e** and **12d**. Nevertheless, this discrepancy may be resolved by considering the fact that it is easier for compound **12c** with the catechol moiety to make a hydrophilic bond *via* π–π stacking than for compound **16k** with the Aβ(1-42) peptide.

We then investigated the effect of the alkyl chain length on the alkoxy moiety. The activity of caffeic acid alkyl esters was enhanced in accordance with the elongation of alkyl chain in the 1 to 5 range. The activity was maximum at the C5-ester (**16d**, EC_{50} = 2.58 µM) and then decreased gradually. Thus, the length of the alkyl side chain (length of the liphophilic moiety) was important for the activity.

The effect of the unsaturated C–C bond in the linker that connected the two catechols was investigated. Comparison of compounds **11a, 12a,** and **c** with the α,β-unsaturated ester and compounds **13a, b,** and **c** with the saturated ester showed that the activities of the corresponding compounds were almost equivalent. This suggested that the unsaturated bond in the linker was not important for the activity.

The mode of connection linking the two catechols was then investigated. The activity of compounds **21a** (69.0 µM) and **21b** (11.4 µM) that connected the carboxyl and alkoxy group *via* the amide were significantly impaired compared to the corresponding ester compounds **12c** and **16d**. On the other hand, the activity of ketone **19** (2.82 µM) was almost equivalent to that of compound **16d**. These results suggested that the resonance effect of amide nitrogen may fix the conformation and affect the activity.

2.3 Kinetics of Aβ(1-42) aggregation in the existence of inhibitors

The aggregation of Aβ(1-42) was followed by an increase in the standard deviation (SD) value of fluorescence intensities owing to the variability of QDAβ(1-42) in coaggregates. The representative aggregation curve on Fig. 2 demonstrates a good fit between the Boltzmann equation used for fitting and experimental data that is confirmed by plotting the residuals versus time in the inset. Parallel measurements at 37°C with 30 µM Aβ(1-42) showed good reproducibility of the maximal SD of fluorescence 6.77 and the aggregation growth rate ($k = 0.533$ min^{-1}) in the control (without inhibitor). The lag time of the reaction was 4.44 min. By contrast, by the addition of 20.3 µM (EC$_{50}$) of rosmarinic acid (**1**) or 5.13 µM of C6-ester (**16e**), the maximal SD of fluorescence was 3.40 and 3.68 and the aggregation growth rate ($k = 0.508$ and 0.190 min^{-1}), without any change in the lag-period of the reaction, respectively. These results demonstrated that the existence of rosmarinic acid (**1**) did not affect the aggregation rate but reduced the total amount of aggregates and extended the lag time (5.58 min). On the contrary, the existence of C6-ester (**16e**) reduced the aggregation rate, the total amount of aggregates and lag-period (1.10 min). Thus, it was suggested that the mechanism of inhibition of rosmarinic acid (**1**) and C6-ester (**16e**) was different.
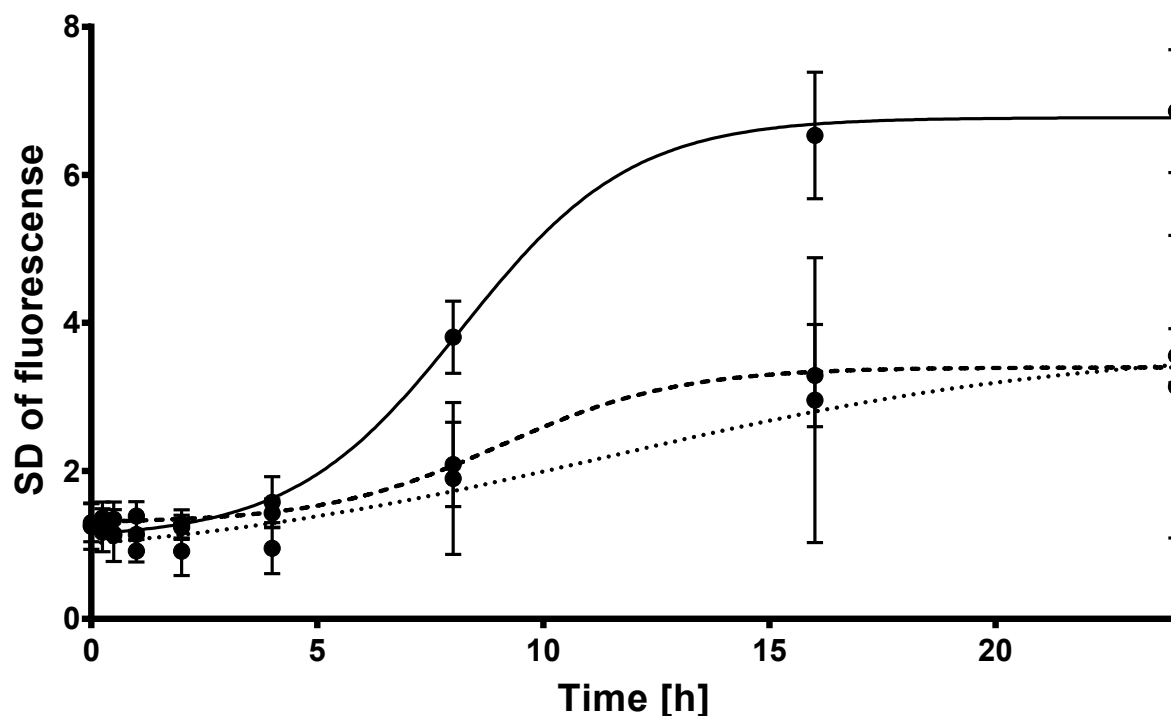
Fig. 2 Time-lapse analyses of process of Aβ(1-42) aggregation with/without 20.3 μM (EC$_{50}$) of rosmarinic acid (**1**) or 5.13 μM of C6-ester (**16e**) obtained by MSHTS system. –•–: control, ---•---: rosmarinic acid (**1**), ⋯•⋯: C6-ester (**16e**)

2.4 CLogP values of rosmarinic acid derivatives

For exhibiting central nervous system (CNS) activity, compounds need to pass through the blood–brain barrier (BBB). One of the factors relevant to success of CNS drugs is lipophilicity. In the common logarithm of octanol/water partition coefficient (cLogP) that showed the degree of calculated lipophilicity from chemical structure, CNS drugs showed significantly higher value than that of peripheral drugs. The average cLogP value of existing CNS drugs was 3.43 [25]. ClogP values of the compounds were shown in Table 1. On comparing the EC$_{50}$ values and cLogP values, the active compounds (**12a**, **12d**, **13b**, **16d**, **16e**, **19**) tended to show suitable cLogP values (3.30, 3.30, 3.11, 3.32, 3.85, 3.53, respectively). Thus, these compounds were expected to show the Aβ(1-42) aggregation inhibitory activity also *in vivo*.

2.5 Docking simulation between rosmarinic acid derivatives and Aβ(1-42) monomer

Clarifying the binding site of rosmarinic acid derivatives on Aβ(1-42), we would be able to presume important amino acid residues in Aβ(1-42) for aggregation and to design more effective inhibitors. Thus, docking simulation between Aβ(1-42) monomer (PDB: 1Z0Q)[26] and 25 of rosmarinic derivatives were performed using AutoDock [27,28].

The results were shown in S-1. Concerning the lowest energy cluster in 50 calculated clusters for each derivatives, the derivatives could be classified in three groups by the activity and binding site: 1) derivatives with $EC_{50} \leqq 10$ µM tended to bind to amide NH and carboxylate in Ala42 with their phenolic hydroxyls *via* hydrogen bond (Fig. 3A); 2) derivatives with 10 µM $< EC_{50} < 100$ µM tended to bind to amide carbonyl oxygen in Ala30 with their phenolic hydroxyl *via* hydrogen bond (Fig. 3B); 3) derivatives with $EC_{50} \geqq 100$ µM tended to bind to side chain in His14 with their ester functional group *via* hydrogen bond (Fig. 3C). Concerning this result that higher effective derivatives tended to bind Ala42 with the report that Aβ(1-42) might aggregate faster than Aβ(1-40) [29], it was suggested that Ala42 played an important role in their aggregation process.

A) 16d (EC$_{50}$ = 2.58 μM)

Leu34
Ala30
Ile31
Met35
Gly38
Ile41
Val40
Val39
Ala42

B) 16b (EC$_{50}$ = 24.7 μM)

Ala30
Ile32
Leu34
Ile31
Met35
Val36
Gly38
Val39

C) 11a (EC$_{50}$ = 1,040 μM)

Hydrogen bond

His6
Asp7
Tyr10
Glu11
His14
Gln15
Val18

N-terminal

C-terminal
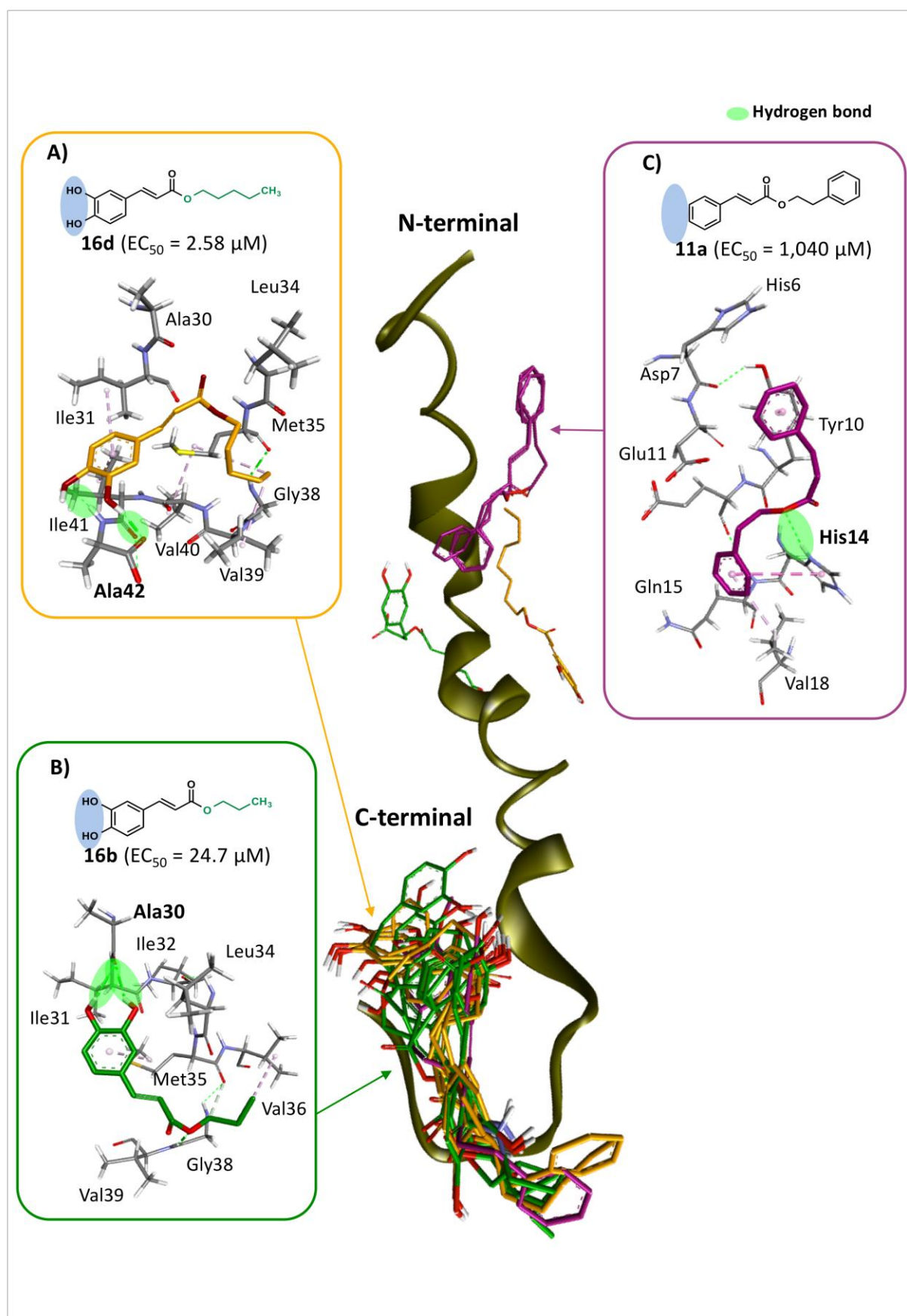
(2 column fitting image)

Fig. 3. Docking model between Aβ(1-42) monomer and rosmarinic acid derivatives calculated by AutoDock.

2.6 XOD inhibitory effect

Among the 25 tested rosmarinic acid derivatives (Table 2), 10 displayed XOD inhibitory potencies. Compounds **2, 12c, 12d, 14, 16b, 16c, 16d, 16j, 16k, 19** showed better potencies. A detailed evaluation of the chemical structures of the active rosmarinic acid derivatives showed a general requirement for two or three hydrophilic moieties for better potency with compounds **2, 12c, 16i, k** being the potent inhibitors in the tested compounds. Additionally, the activity of series of caffeic acid alkyl esters were depending on the length of alkyl side chain. Most potent derivatives were compound **16c** and **16d** (butyl and pentyl ester).

Table 2. XOD inhibitory and DPPH radical-scavenging activity

compound	XOD inhibition (%)			DPPH radical scavenging activity (%)	
	1 μM	10 μM	100 μM	100 μM	500 μM
1		< 10	27	47	66
2		38	82	39	48
3		< 10	< 10	49	63
8f		< 10	65	48	64
11a		< 10	< 10	< 10	< 10
12a		< 10	22	40	56
12b		50	43	43	59
12c		26	80	37	46
12d		< 10	62	35	51
13a		< 10	< 10	< 10	< 10
13b		< 10	< 10	38	54
13c		< 10	21	37	49
13d		< 10	< 10	< 10	< 10
16a		< 10	22	46	62
16b		< 10	61	46	63
16c		<10	> 90	46	62
16d		11	> 90	46	62
16e		10	< 10	45	61
16f		11	25	46	63

16g		< 10	40	45	61
16i		< 10	84	41	54
16k		< 10	51	42	55
19		12	76	48	62
21a		< 10	30	47	64
21b		< 10	33	40	53
allopurinol	< 10	> 90			
edaravone				50-53	71-75

2.7 Antioxidant ability (DPPH radical scavenging assay)

The antioxidant activities of rosmarinic acid derivatives were based on their interaction with the 2,2-diphenyl-1-picrylhydrazyl (DPPH) free radical (Table 2) [30]. As expected, the results suggested that compounds without catechol type aromatic ring did not exhibit significant antioxidant activities, as it is shown by the low inhibition percentages at very high concentrations (<10% at 500 µM concentration). Thus, the significant radical scavenging activity of the tested compounds can be explained by the presence of catechol phenolic hydroxyls that are important in the scavenging action of ROS species. However, we could not find a specific structural feature of caffeic acid-type compounds is present in all the compounds, and caffeic acid itself has significant antioxidant activity.

3. Conclusions

In summary, rosmarinic acid derivatives were synthesized and their Aβ(1-42) aggregation inhibitory activity was investigated. After detailed consideration of structure–activity relations, it was suggested that the structural requirement of rosmarinic acid derivatives to express the activity was phenolic hydroxyls in unilateral side and the length of the alkoxy moiety.

Additionally, normally ester functional group was labile intravitally to hydrolases to metabolite to carboxylic acid and alcohol. Thus, the fact that compound **19** showed the equivalent activity to compound **16d** gave us hope to develop *in vivo* experiment.

Docking simulation of Aβ(1-42) monomer and rosmarinic acid derivatives by AutoDock suggested that potent Aβ aggregation inhibitor tend to dock the Ala42, Ile31, and Val39. This result suggested the importance of C-terminal of Aβ(1-42) for the aggregation. XOD inhibitory effect was affected by the compounds lipophilicity. DPPH antioxidation activity was found in the derivatives with catechol type moiety.

The present study sheds new light on the properties of this interesting group of compounds. Further studies are now underway in our laboratory, including a search for more effective analogs and

studies exploring the mechanism of action of these compounds.

4. Experimental Part

4.1 MSHTS system

The EC_{50} values of compounds were determined by a modified MSHTS system [12]. More specifically, various concentrations of rosmarinic acid derivatives, 30 nM QD - labeled Aβ(1-42) (QDAβ(1-42)), and 30 μM Aβ(1-42) in PBS containing 5% EtOH and 3% DMSO were incubated in a 1536 - well plate at 37°C for 24 h, and the formed QDAβ(1-42)–Aβ(1-42) coaggregates in each well were observed by an inverted fluorescence microscope equipped with a color CCD camera. SD values of fluorescence intensities of 10,000 pixels (100 × 100 pixels: 167 × 167 mm) in the central region of each well were measured by the ImageJ software. The SD values, which were approximately proportional to the amount of aggregates, were plotted against the concentrations of added rosmarinic acid derivatives to establish an inhibition curve. EC_{50} values were estimated from the inhibition curve using the EC_{50} shift by the Prism global fitting software.

4.2 Data analysis and kinetic formation

The kinetics of Aβ(1-42) aggregation could be described as sigmoid curves, and aggregation parameters were determined by fitting the plot of the SD values of fluorescence intensities versus time in the Boltzmann equation.

$$SD = \frac{SD_{max}-SD_{min}}{1-exp\{(t_{50}-t)k\}},$$

where SD_{min} is the initial SD level, SD_{max} is SD of maximal aggregation level, t_{50} is the time when fluorescence reaches half maximal, and k is the rate constant of aggregate formation. The lag time is calculated as

$$lag = t_{50} - 2/k$$

4.2 Molecular Docking [27,28]

AutoDock, PytonMolecularViewer, and Cygwin were used for the docking simulation of interactions between Aβ(1-42) and inhibitors. ChemBioDraw was used for the preparation of chemical structure data of inhibitors for the docking simulation. ChemBio3D was used for the calculation of molecular dynamics and the most stable conformation of inhibitors. The results of docking simulation were analyzed by using Discovery Studio. PDB: 1Z0Q [26] was used for the docking simulation with Aβ(1-42) aggregation inhibitors. The compounds used for the docking simulation were 25 rosmarinic acid derivatives.

4.3 XOD inhibition test

35 µL of phosphate buffer (100 mM, pH=7.6), 50 µL of a solution of allopurinol and rosmarinic acid derivatives in DMSO, 30 µL of a solution of XOD (from butter milk, Oriental Yeast Co., Ltd.) in phosphate buffer were added in 96 well micro plate. Then, 60 µL of a solution of 500 µM xanthine in phosphate buffer was added to the solution at rt. After 8 min, 1N HClaq was added and absorbance at 290 nm was measured. The inhibition rate (%) was calculated according to the following equation:

$$Inhibition\ rate\ (\%) = \left[1 - \frac{Abs(XOD\ inhibition\ activity) - Abs(sample)}{(Abs(XOD\ activity) - Abs(Blank))}\right] \times 100$$

4.4 1,1-Diphenyl-2-picrylhydrazyl (DPPH) radical scavenging assay

40 µL of 1 mM DPPH solution and 150 µL of EtOH were added to 96 well plate. Then, 10 µL of 2 mM or 10 mM of edaravone, or rosmarinic acid derivatives in DMSO was added at rt. And then, the absorbance at 517 nm was continuously measured for 60 min, and radical trapping capacity was calculated with the data at 20 min following the equation:

$$DPPH\ radical\ trapping\ capacity\ (\%) = \left\{\left(\frac{Abs(20\ min) - Abs(sample)}{Abs(DPPH) - Abs(blank)}\right)\right\} \times 100$$

4.5 Typical reaction procedure for the construction of rosmarinic acid derivatives (12c)

4.5.1 Methyl caffeate (**4**)

A mixture of caffeic acid (309.2 mg, 1.72 mmol), EDCI (385.3 mg, 2.01 mmol) and DMAP (22.1 mg, 0.181 mmol) in methyl alcohol (400 µL) was stirred at 60°C for 13 h. The resulting mixture was quenched with 2N HCl and extracted with AcOEt. The combined organic phases were washed with sat. NaHCO$_3$, dried over anhydrous magnesium sulfate, and evaporated under reduced pressure. The residue was purified by column chromatography on silica gel (MeOH–CHCl$_3$) (1:5 v/v) to give a title compound (287.5 mg, 86%) as a white solid. Mp: 161°C–164°C [31], IR ṽ: 3489, 3303, 2955, 2925, 1679, 1601, 1519 cm^{-1}. ^{1}H-NMR (500 MHz, acetone-d_6) δ: 7.51 (d, 1H, J = 16.1 Hz), 7.13 (d, 1H, J = 2.0 Hz), 7.02 (dd, 1H, J = 2.0, 8.0 Hz), 6.84 (d, 1H, J = 8.0 Hz), 6.26 (d, 1H, J = 16.1 Hz), 3.69 (s, 3H). ^{13}C-NMR (125 MHz, acetone-d_6) δ: 167.0, 147.9, 145.5, 144.9, 126.8, 121.7, 115.6, 114.5, 114.4. High-resolution MS calcd. for C$_{10}$H$_{10}$O$_4$ (M$^+$): 194.0579. Found: 194.0585. All spectral data agreed with previously reported data [32].

4.5.2 Methyl 3,4-bis[[(2-nitrophenyl)sulfonyl]oxy] cinnamate (**5**)

To a solution of **4** (194.6 mg, 1.00 mmol) in CH$_3$CN (2.2 mL) were added triethylamine (0.63 mL, 4.50 mmol) and 2-nitrobenzenesulfonyl chloride (487.1 mg, 2.30 mmol) at 0°C. The mixture was stirred at 0°C for 0.5 h. The reaction mixture was quenched with 2M HCl and extracted with

CH_2Cl_2. The combined organic phases were washed with brine, dried over anhydrous magnesium sulfate and evaporated under reduced pressure. The residue was purified by column chromatography on silica gel (AcOEt–n-hexane) (3:2 v/v) to give a title compound (562.9 mg, 99%) as white solid. Mp: 118°C–123°C, IR ṽ: 3099, 1714, 1542, 1390, 1191, 850, 814, 693 cm^{-1}. ^{1}H-NMR (500 MHz, CDCl$_3$) δ: 8.03 (dd, 2H, J = 1.3, 7.9 Hz), 7.89–7.84 (m, 2H), 7.81–7.74 (m, 4H), 7.58 (d, 11H, J = 16.0 Hz), 7.48 (dd, 1H, J = 2.0, 8.5 Hz), 7.45 (d, 1H, J = 2.0 Hz), 7.36 (d, 1H, J = 8.5 Hz), 6.39 (d, 1H, J = 16.0 Hz), 3.82 (s, 3H). ^{13}C-NMR (125 MHz, CDCl$_3$) δ: 166.4, 148.2, 148.1, 141.6, 141.4, 141.1, 136.0, 135.1, 132.5, 131.6, 128.2, 128.1, 127.8, 124.9, 123.4, 120.7, 51.8.

4.5.3 3,4-Bis[(2-nitrophenyl)sulfonyl]oxycinnamic acid (6)

To a solution of **5** (113.3 mg, 0.20 mmol) in AcOH (3.1 mL) was added 0.5M HCl aq (3.1 mL) at 0°C. The mixture was stirred at 85°C for 37 h. The reaction mixture was added H_2O and extracted with AcOEt. The combined organic phases were washed with brine, dried over anhydrous magnesium sulfate and evaporated under reduced pressure. The residue was purified by column chromatography on silica gel (MeOH–CHCl$_3$) (1:20 v/v) to give a title compound (110.4 mg, 99%) as white solid. Mp: 182°C–186°C, IR ṽ: 3104, 1687, 1544, 1378, 1355, 1180, 1124, 851, 821, 721 cm^{-1}. ^{1}H NMR (500 MHz, acetone-d_6): δ 8.12–8.04 (m, 6H), 7.97–7.92 (m, 2H), 7.79 (dd, 1H, J = 2.1, 8.6 Hz), 7.67 (d, 1H, J = 2.1 Hz), 7.64 (d, 1H, J = 16.0 Hz), 7.41 (d, 1H, J = 8.6 Hz), 6.55 (d, 1H, J = 16.0 Hz). ^{13}C-NMR (125 MHz, acetone-d_6) δ: 167.1, 148.49, 148.77, 142.3, 142.0, 141.8, 137.3, 136.1, 133.44, 133.40, 132.1, 128.8, 128.0, 125.8, 125.5, 125.3, 124.3, 121.9, 78.7. High-resolution MS calcd for $C_{21}H_{14}N_2O_{12}S_2$ (M$^+$): 549.9988. Found: 549.9969.

4.5.4 Allyl (3,4-dihydroxyphenyl)acetate (8)

To a mixture of (3,4-dihydroxyphenyl)acetic acid (**7**, 1.01 g, 6.02 mmol), EDCI (1.38 g, 7.21 mmol) and DMAP (73.4 mg, 0.60 mmol) was added allyl alcohol (4.5 mL) at room temperature, then heated at 60°C for 2 h. The resulting mixture was quenched with 2N HCl and extracted with AcOEt. The combined organic phases were washed with sat. NaHCO$_3$, dried over anhydrous magnesium sulfate and evaporated under reduced pressure. The residue was purified by column chromatography on silica gel (acetone–n-hexane) (1:5 v/v) to give a title compound (1.11 g, 89%) as yellow oil. IR ṽ: 3389, 1706, 1606, 1281, 988, 961, 795 cm^{-1}. ^{1}H NMR (500 MHz, acetone-d_6): δ 6.77 (d, 1H, J = 2.2 Hz), 6.73 (d, 1H, J = 8.2 Hz), 6.59 (dd, 1H, J = 2.2, 8.2 Hz), 5.93–5.85 (m, 1H), 5.24 (dq, 1H, J = 1.6, 17.3 Hz), 5.13 (dq, 1H, J = 1.6, 10.6 Hz), 4.52 (dt, 2H, J = 1.6, 5.5 Hz), 3.47 (s, 2H). ^{13}C NMR (125 MHz, acetone-d_6): δ 171.8, 145.6, 144.8, 133.5, 126.7, 121.5, 117.7, 117.1, 115.9, 65.4, 40.8. High-resolution MS calcd for $C_{11}H_{12}O_4$ (M$^+$): 208.0736. Found: 208.0727.

4.5.5 Allyl [3,4-bis(*tert*-butyldimethylsilyl)oxyphenyl]benezeneacetate (**9**)

To a solution of compound **8** (1.06 g, 5.11 mmol), TBSCl (1.86 g, 12.3 mmol) and imidazole (1.75 g, 25.7 mmol) in DMF (2.3 mL) was stirred at 0°C for 0.5 h. The reaction mixture was added sat. NH_4Cl and extracted with AcOEt. The combined organic phases were washed with sat. $NaHCO_3$ and brine, dried over anhydrous magnesium sulfate, and evaporated under reduced pressure. The residue was purified by column chromatography on silica gel (AcOEt–*n*-hexane) (1:20 *v/v*) to give a title compound (2.16 g, 97%) as colorless oil. IR $\tilde{v}$: 2930, 1739, 1228, 905, 836 cm^{-1}. ^{1}H NMR (500 MHz, $CDCl_3$): δ 6.79 (d, 1H, J = 2.0 Hz), 6.76 (d, 1H, J = 8.0 Hz), 6.71 (dd, 1H, J = 2.0, 8.0 Hz), 5.91–5.84 (m, 1H), 5.24 (dq, 1H, J = 1.6, 17.2 Hz), 5.18 (dq, 1H, J = 1.3, 10.1 Hz), 4.58 (dt, 2H, J = 1.4, 5.7 Hz), 3.51 (s, 2H), 0.99 (s, 9H), 0.98 (s, 9H), 0.193 (s, 6H), 0.188 (s, 6H). ^{13}C NMR (125 MHz, $CDCl_3$): δ 171.5, 146.8, 146.1, 132.2, 127.0, 122.3, 122.2, 121.0, 118.2, 65.4, 40.8, 26.0, 18.5, −4.0. High-resolution MS calcd for $C_{23}H_{40}O_4Si_2$ (M$^+$): 436.2466. Found: 436.2463.

4.5.6 2-[3,4-bis(*tert*-butyldimethylsilyl)oxyphenyl]ethanol (**10a**)

To a suspension of $LiAlH_4$ (278.9 mg, 4.90 mmol) in THF (2.00 mL) at 0°C were added compound **9** (2.13 g, 4.88 mmol) in THF (17.5 mL). The reaction mixture was stirred at room temperature for 0.5 h. The mixture was filtered through a Celite pad and evaporated under reduced pressure. The residue was purified by column chromatography on silica gel (AcOEt–*n*-hexane) (1:4 *v/v*) to give a title compound (1.83 g, 98%) as colorless oil. IR $\tilde{v}$: 3326, 2929, 1463, 980, 834 cm^{-1}. ^{1}H NMR (500 MHz, $CDCl_3$): δ 6.69 (d, 1H, J = 8.3 Hz), 6.62 (d, 1H, J = 2.0 Hz), 6.58 (dd, 1H, J = 2.0, 8.3 Hz), 3.70 (t, 2H, J = 6.5 Hz), 2.66 (t, 2H, J = 6.5 Hz), 0.92 (s, 9H), 0.91 (s, 9H), 0.121 (s, 6H), 0.117 (s, 6H). ^{13}C NMR (125 MHz, $CDCl_3$): δ 146.7, 145.4, 131.3, 121.84, 121.79, 120.1, 63.7, 38.5, 25.8, 18.4, −4.1. High-resolution MS calcd for $C_{20}H_{38}O_3Si_2$ (M$^+$): 382.2360. Found: 382.2370.

4.5.7 2-[3,4-bis(*tert*-butyldimethylsilyl)oxyphenyl]ethyl 3,4-bis[[(2-nitrophenyl)sulfonyl]oxy]cinnamate (**11d**)

To a cooled (0°C) solution of **6a** (278.5 mg, 0.51 mmol) and **10a** (118.7 mg, 0.31 mmol) in dry THF (1.6 mL) were added PPh$_3$ (205.5 mg, 0.78 mmol) and DEAD (0.12 mL, 0.78 mmol). The reaction mixture was stirred at room temperature for 21 h. Then, the reaction was worked up by removal of the solvent, redissolved on AcOEt, and extracted with sat. $NaHCO_3$. The organic phase was washed with brine, dried over anhydrous magnesium sulfate, and evaporated under reduced pressure. The residue was purified by column chromatography on silica gel (AcOEt–CHCl$_3$) (1:30 *v/v*) to give a title compound (266.1 mg, 94%) as yellow-green solid. Mp: 57°C–61°C, IR $\tilde{v}$: 2930, 2858, 1714, 1544, 1471, 1391, 1193, 1128, 903, 827, 781 cm^{-1}. ^{1}H NMR (500 MHz, $CDCl_3$): δ

8.04–8.01 (m, 2H), 7.88–7.84 (m, 2H), 7.80–7.73 (m, 4H), 7.55 (d, 1H, J = 16.1 Hz), 7.47–7.45 (m, 2H), 7.35 (d, 1H, J = 8.3 Hz), 6.77 (d, 1H, J = 8.2 Hz), 6.71 (d, 1H, J = 2.3 Hz), 6.68 (dd, 1H, J = 2.3, 8.2 Hz), 6.37 (d, 1H, J = 16.1 Hz), 4.36 (t, 2H, J = 7.0 Hz), 2.88 (t, 2H, J = 7.0 Hz), 0.981 (s, 9H), 0.979 (s, 9H), 0.192 (s, 6H), 0.189 (s, 6H). ^{13}C NMR (125 MHz, CDCl$_3$): δ 165.8, 148.2, 148.1, 146.5, 245.4, 141.6, 141.3, 141.1, 135.9, 135.1, 132.4, 131.7, 130.6, 128.2, 128.2, 127.8, 124.9, 1247, 123.4, 121.7, 121.6, 121.0, 120.965.5, 34.3, 25.8, 18.3, −4.2.

4.5.8 2-(3,4-Dihydroxyphenyl)ethyl caffeate (12c)

2-[3,4-bis(*tert*-butyldimethylsilyloxy)phenyl]ethyl caffeate

To a suspension of Cs$_2$CO$_3$ (1.19 g, 3.55 mmol) in CH$_3$CN (1.90 mL) were added thiophenol (0.18 mL, 1.79 mmol) and **11d** (132.2 mg, 0.14 mmol) at 0°C. The mixture was stirred at room temperature for 1.5 h. The reaction was quenched with sat. NH$_4$Cl and extracted with AcOEt. The organic phase was dried over anhydrous magnesium sulfate and evaporated under reduced pressure. The residue was purified by column chromatography on silica gel (MeOH–CHCl$_3$) (1:100 *v/v*) to give a title compound (64.6 mg, 82%) as yellow-green solid. Mp: 130°C–134°C, IR ṽ: 3463, 2929, 1670, 1278, 980, 906, 836, 782 cm^{-1}. ^{1}H NMR (500 MHz, CDCl$_3$): δ 7.56 (d, 1H, J = 16.1 Hz), 7.08 (s, 1H), 7.60 (dd, 1H, J = 2.0, 8.0 Hz), 6.87 (d, 1H, J = 8.0 Hz), 6.76 (d, 1H, J = 8.0 Hz), 6.72 (d, 1H, J = 2.0 Hz), 6.68 (dd, 1H, J = 2.0, 8.0 Hz), 6.25 (d, 1H, J = 16.1 Hz), 4.34 (t, 2H, J = 7.0 Hz), 2.89 (t, 1H, J = 7.0 Hz), 0.98 (s, 18H), 0.19 (s, 12H). ^{13}C NMR (125 MHz, CDCl$_3$): δ 167.7, 146.6, 146.3, 145.5, 150.0, 143.7, 130.8, 127.5, 122.4, 121.8, 121.7, 121.0, 115.6, 115.5, 114.4, 65.4, 34.5, 25.9, 18.4, −4.1. High-resolution MS calcd for C$_{29}$H$_{44}$O$_6$Si$_2$ (M$^+$): 544.2677. Found: 544.2688.

To a solution of above compound (60.4 mg, 0.11 mmol) in THF (3.6 mL) were added TBAF (1.1 M in THF) (0.40 mL, 0.44 mmol) at 0°C. The mixture was stirred at room temperature for 2.5 h. Then, the reaction was worked up by removal of the solvent, redissolved on AcOEt, and extracted with H$_2$O. The organic phase was washed with brine, dried over anhydrous magnesium sulfate, and evaporated under reduced pressure. The residue was purified by column chromatography on silica gel (MeOH–CHCl$_3$) (1:20 *v/v*) to give a title compound (29.6 mg, 84%) as white solid. Mp: 118–120 ºC [28], IR ṽ: 3283, 1680, 1394, 1168, 853, 810 cm^{-1}. ^{1}H NMR (500 MHz, MeOH-d_4): δ 7.51 (d, 1H, J = 15.7 Hz), 7.02 (d, 1H, J = 2.0 Hz), 6.92 (dd, 1H, J = 2.0, 8.0 Hz), 6.76 (d, 1H, J = 8.0 Hz), 6.70–6.68 (m, 2H), 6.56 (dd, 1H, J = 2.0, 8.0 Hz), 6.23 (d, 1H, J = 15.7 Hz), 4.27 (t, 2H, J = 7.2 Hz), 2.82 (t, 2H, J = 7.2 Hz). ^{13}C NMR (125 MHz, MeOH-d_4): δ 169.3, 149.5, 146.9, 146.8, 146.2, 145.0, 144.9, 130.8, 127.7, 123.0, 121.2, 117.0, 116.5, 116.4, 115.1, 66.5, 35.6. High-resolution MS calcd for C$_{17}$H$_{16}$O$_4$ (M$^+$): 316.0947. Found: 316.0962. All spectral data agreed with previously reported data [33].

4.6 Calculation of cLogP value of tested compounds

CLogP values of synthesized compounds were calculated using ChemBio3D Ultra 12.0 (PerkinElmer).

References

[1] C. R. Jack Jr., D. S. Knopman, W. J. Jagust, L. M. Shaw, P. S. Aisen, M. W. Weiner, R. C. Petersen, J. Q. Trojanowski, Hypothetical model of dynamic biomarkers of the Alzheimer's pathological cascade, Lancet Neurol. 9 (2010) 119-128.

[2] H. Hanyu, Lifestyle-related desease and dementia, Dementia Japan 30 (2016) 317-318.

[3] S. Gauthier, Alzheimer's disease: current and future therapeutic perspectives, Prog. Neuropsychopharmacol. Biol. Psychiatry 25 (2001) 73-89.

[4] J. A. Hardy, G. A. Higgins, Alzheimer's disease: the amyloid cascade hypothesis, Science 256 (1992) 184-185.

[5] Y. Zhou, C. Jiang, Y. Zhang, Z. Liang, W. Liu, L. Wang, C. Luo, T. Zhong, Y. Sun, L. Zhao, X. Xie, H. Jiang, N. Zhou, D. Liu, H. Liu, Structural optimization and biological evaluation of substituted bisphenol a derivatives as β-amyloid peptide aggregation inhibitors, J. Med. Chem. 53 (2010) 5449-5466.

[6] A. F. McKoy, J. Chen, T. Schupbach, M. H. Hecht, Structure-activity relationships for a series of compounds that inhibit aggregation of the Alzheimer's peptide, Aβ42, Chem. Biol. Drug. Design. 84 (2014) 505-512.

[7] M. Necula, R. Kayed, S. Milton, C. G. Glabe, Small molecule inhibitors of aggregation indicate that amyloid β oligomerization and fibrillization pathways are independent and distinct, J. Biol. Chem. 287 (2007) 10311-10324.

[8] T. Arai, A. Ohno, K. Mori, T. Kakizawa, H. Kuwata, T. Ozawa, M. Shibanuma, S. Hara, S. Ishida, M. Kurihara, N. Miyata, H. Nakagawa, K. Fukuhara, Design, synthesis, and evaluation of Trolox-conjugated amyloid-β C-terminal peptides for therapeutic intervention in an in vitro model of Alzheimer's disease, Bioorg. Med. Chem. 24 (2016) 4138-4143.

[9] K. Murakami, K. Irie, H. Ohigashi, H. Hara, H.; Nagao, M.; Shimizu, T.; Shirasawa, Formation and stabilization model of the 42-mer Abeta radical: implications for the long-lasting oxidative stress in Alzheimer's disease, J. Am. Chem. Soc. 127 (2005) 15168-15174.

[10] D. Yanagisawa, H. Taguchi, S. Morikawa, T. Kato, K. Hirao, N. Shirai, I. Tooyama, Novel curcumin derivatives as potent inhibitors of amyloid ☐ aggregation, Biochem. Biophys. Rep. 4 (2015) 357-368.

[11] H. Endo, Y. Nikaido, M. Nakadate, S. Ise, H. Konno, Structure activity relationship study of curcumin analogues toward the amyloid-beta aggregation inhibitor, Bioorg. Med. Chem. Lett. 24 (2014) 5621-5626.

[12] Y. Ishigaki, H. Tanaka, T. Ogara, K. Uwai, K. Tokuraku, A microliter-scale high-throughput screening system with quantum-dot nanoprobes for amyloid-β aggregation inhibitors, PLoS. ONE. 8 (2013) e72992.

[13] T. Hamaguchi, K. Ono, A. Murase, M. Yamada, Phenolic compounds prevent Alzheimer's pathology through different effects on the amyloid-beta aggregation pathway, Am. J. Pathol. 175 (2009) 2557-2565.

[14] J. H. Chen, C.-T. Ho, Antioxidant activities of caffeic acid and its related hydroxycinnamic acid compounds, J. Agric. Food. Chem. 45 (1997) 23742378.

[15] A. Kern, C. Behl, The unsolved relationship of brain aging and late-onsetAlzheimer disease. Biochim. Biophys. Acta 1790 (2009) 1124–1132.

[16] S. J. Yang, W. J. Lee, E. A. Kim, K. D. Nam, H. G. Hahn, S. Y. Choi, S. W. Cho, Effects of N-adamantyl-4-methylthiazol-2-amine on hyperglycemia, hyperlipidemia and oxidative stress in streptozotocin-induced diabetic rats. Eur. J. Pharmacol. 736 (2014) 26–34.

[17] X.-L. Bu, P. P. N. Rao, Y.-J. Wang, Anti-amyloid aggregation activity of natural compounds: implications for Alzheimer's drug discovery, Mol. Neurobiol. 53 (2016) 3565-3575.

[18] J. Won, Y.-G. Hur, S.-J. Kim, S.-H. Park, D. Park, Pharmaceutical composition comprising hydroxylphenyl derivatives of rosmarinic acid for anticancer, WO 2005072723 A1 2005-08-11.

[19] J. Won, K. Lee, S. Park, S.-J. Kim, S.-Y. Yun, M.-A. Kang, T.-G. Hur, J. Youn, Y. Yun, D. Park, D., Derivatives of Hydroxyphenyl, A Method for Preparing Thereof and Their Pharmaceutical Composition, WO 2003089405 A1 2003-10-30.

[20] Y. Liu, X. Li, D.-C. Xiong, B. Yu, X. Pu, X.-S. Ye, Synthetic Phenylethanoid Glycoside Derivatives as Potent Neuroprotective Agents, Eur. J. Med. Chem. 95 (2015) 313-312.

[21] Z. Zhang, B. Xiao, Q. Chen, X.-Y. Lian, Synthesis and Biological Evaluation of Caffeic Acid 3,4-Dihydroxyphenethyl Ester, J. Nat. Prod. 73 (2010) 252-254.

[22] S. Okombi, D. Rival, A. Boumendjel, A.-M. Mariotte, E. J. L. Perrier, Use of p-Hydroxycinnamic acid derivatives in cosmetic or dermatological compositions, GB 2431876 A 2007-05-09.

[23] Z. N. Kayani, R. A. Lewis, S. Naseem, Development of novel chiral dopants to be used in ferroelectric liquid crystal system, J. Mol. Liq. 180 (2013) 74-88.

[24] Y. Zhu, A. Mohammadi, J. Ralph, Facile synthesis of 4-hydroxycinnamaldehydes, Bioenerg. Res. 5 (2012) 407-411.

[25] M. S. Alavijeh, M. Chishty, M. Z. Qaiser, A. M. Palmer, Drug metabolism and pharmacokinetics, the blood-brain barrier, and central nervous system drug discovery, NeuroRx. 2 (2005) 554-571.

[26] The RCSB PDB. http://www.rcsb.org/pdb/home/home.do

[27] Auto Dock. http://autodock.scripps.edu/

[28] S. M. D. Rizvi, S. Shakil, M. Haneef, A simple click by click protocol to perform docking: Autodock 4.2 made easy for *non*-bioinformaticians, EXCLI J., 12 (2013) 831-857.

[29] G. K. Gouras, J. Tsai, J. Naslund, B. Vincent, M. Edgar, F. Checler, J. P. Greenfield, V. Haroutunian, J. D. Buxbaum, H. Xu, P. Greengard, N. R. Relkin, N. R., Intraneuronal Abeta42 accumulation in human brain, Am. J. Pathol. 156 (2000) 15-20.

[30] B. Tepe, D. Daferera, A. Sokmen, M. Sokmen, M. Polissiou, Antimicrobial and antioxidant activities of the essential oil and various extracts of Salvia tomentosa Miller (Lamiaceae), Food Chem. 90 (2005) 333-340.

[31] K. Ohara, Y. Ichimura, S. Nagaoka, Kinetic study of singlet-oxygen quenching by cffeic acid and related phenols, Bull Chem Soc Jpn, 82, (2009) 689-691.

[32] K. Uwai, Y. Osanai, T. Imaizumi, S. Kanno, M. Takeshita, M. Ishikawa, Inhibitory effect of the alkyl side chain of caffeic acid analogues on lipopolysaccharide-induced nitric oxide production in RAW264.7 macrophages, Bioorg. Med. Chem. 16 (2008) 7795-7803.

[33] L. Chapado, P. J. Linares-Palomino, S. Salido, J. Altarejos, J. A. Rosado, G. M. Salido, G. M., Synthesis and evaluation of the platelet antiaggregant properties of phenolic antioxidants structurally related to rosmarinic acid, Bioorg Chem, 38 (2010) 108-114.